J Mol Model (2006) 12: 406–410
DOI 10.1007/s00894-005-0060-4

ORIGINAL PAPER

Shi-Ling Yuan · Xiu-Qing Zhang · Gui-Ying Xu · Dong-Ju Zhang

Mesoscopic simulation study on a weakly charged block polyelectrolyte in aqueous solution

Received: 18 February 2005 / Accepted: 12 July 2005 / Published online: 16 December 2005

Abstract In this paper, we use density functional theory to study the effect of the charge of solvophilic beads and concentration on the mesoscale structures of polyelectrolyte solution. The polyelectrolyte $A_6B_{12}A_6$ was selected as the triblock polymer, and the solvophobic B blocks have no charges, while the solvophilic A blocks are charged. The simulation results showed: at higher concentration (above 50% systems), relatively small charges on the solvophilic block do not alter the bicontinuous phase inherent to uncharged solution, but at moderate concentrations (50% system), even though the charge per solvophilic bead is very small, the order lamellar structures become disturbed.

Keywords Polyelectrolyte · Block polymer · Mesoscopic simulation · MesoDyn simulaiotn

Introduction

Polyelectrolyte solutions have been widely investigated in biology and industrial applications in recent decades. Both theoretical [1–4] and experimental [5–8] methods have been selected to study the properties of these solutions. In contrast to the phase behavior of uncharged block copolymer solutions, block-polyelectrolyte solutions are more challenging and difficult to investigate due to the presence of both short-range (excluded volume) and long-range (electrostatic) interactions. [9] Some experiments have shown that block-polyelectrolyte aqueous solutions can form different aggregates such as spherical [6] or cylindrical micelles [7, 8] with a dense hydrophobic core and charged corona. Using theoretical calculations, different micelles of block copolymers with polyelectrolyte and hydrophobic blocks was also discussed *via* a mean-field theory, [10] and a relationship between the parameters of micelles and the fraction of charged monomers was found in dilute aqueous solutions. In contrast to dilute solutions, the situation for concentrated polyelectrolyte solutions is more complicated due to the strong correlation between polymeric domains. [1, 2] Kyrylyuk and Fraaije [9] used MesoDyn density functional theory (MDDFT) to investigate the self-assembly of triblock polymers with a weak polyelectrolyte block in concentrated aqueous solution, and established the phase diagram of the polyelectrolyte in solution as a function of the charge of the solvophilic block and the solvent concentration.

In this paper, we also depict the phase behavior of concentrated block-polyelectolyte solution in the presence of a salt. The morphology of block copolymer in the solution can be studied effectively using MESODYN program [11] in Cerius^2 4.6 by Accelrys. This method is based on MDDFT developed by Fraaije several years ago, [11, 12] and the phase-separation dynamics and ordering processes of multicomponent polymeric systems are described by Langevin equations for mesoscale modeling. One important advantage of this method is that there is no a priori assumption on the phases, [13] and that the kinetics of phase formation, which is very difficult to observe experimentally, can be studied. In the first part of this work, the method and simulated model will be shown simply; then the parameters used in the MESODYN method are explained to show the relationship between parameters and morphology; lastly, the phase diagram of a model triblock polyelectrolyte solution in coordinates of the charge of the polyelectrolyte (solvophilic) block and polymer concentration is obtained through the order parameters of the blocks with increasing concentration of the polymer, and the effect of the charge of block polymers on the morphology of self-assembled systems discussed in the solution.

Materials, methods and models

The basic idea in the MESODYN method is density functional theory. It is based on the idea that the free energy

S.-L. Yuan (✉) · X.-Q. Zhang · G.-Y. Xu · D.-J. Zhang
Key lab of Colloid and Interface Chemistry,
Shandong University,
Jinan, 250100, People's Republic of China
e-mail: shilingyuan@sdu.edu.cn
Fax: +86-531-88564464

F of an inhomogeneous liquid is a function of the local density function ρ. From the free energy, all thermodynamic functions can be derived so that, for instance, phase transitions can be investigated as a function of the density distribution in the system.

To specify the chemical nature of the system in a MESODYN simulation, two sets of parameters must be defined, one is the chain topology in terms of repeat segments (or beads) and the other is the interaction energies of the various types of segments. For the first, this method uses a Gaussian chain description with all segments of the same size, and the chain topology depends on the degree of coarsening of the original system. In this "spring and beads" model, springs mimic the stretching behavior of a chain fragment and different kinds of beads correspond to different components in the block copolymer. In this article, we selected a polyelectrolyte as a triblock polymer. The block polymer is shown in Fig. 1. In our calculation, each bead in the Gaussian chain is a statistical unit, and therefore represents a number of "real" monomers, so the choice of the Gaussian chain is an important aspect of the method. Lam [13] used the Monte Carlo method to obtain a statistical sample of atomistic chains for block polymers, and then obtained the relationship between atomistic chains and Gaussian chains. He used $A_6B_{12}A_6$ (Gaussian chains) to represent the atomistic chains of polymer $PEO_{26}PPO_{40}$ PEO_{26} (P85). In our simulations, we selected the Gaussian chain $A_6B_{12}A_6$ as our polymer to be investigated, and discuss the effect of different charge on the beads on the morphology of polymer. In the block polymer, the solvophobic B blocks have no charges, while the solvophilic A blocks are charged, with z_A being the absolute value of the charge per bead. One bead S represents the solvent molecule in a MesoDyn simulation, and the solvent is assumed to be neutral.

Secondly, the important interaction energies of the various types of segments can be defined by the Flory–Huggins interaction parameters χ among different beads. In fact, these parameters can be considered non-ideal interactions that are included *via* a mean field, and the strength of interaction between different components is characterized by the interaction parameter ε_{AB}, which we express in units of kJ mol^{-1}. A positive ε_{IJ} parameter corresponds to a repulsion between the components I and J. The dynamics of the component densities $\rho_I(r,t)$, with I=A,B, are described by a set of functional Langevin equations. These are diffusion equations of the component densities which take into account the noise in the system. Driving forces for diffusion are local gradients of chemical potentials $\mu_I=\delta F[\{\rho_I\}]/\delta\rho_I$. The Langevin diffusion equations are solved numerically with homogeneous initial conditions. As MESODYN is based on the same type of free energy functional as self-consistent field theory (SCFT), it is expected to approach on long time scales the same solutions as SCFT does by searching for the absolute minimum of the free energy. With MESODYN, however, structure formation proceeds via local gradients of chemical potentials that are intrinsic to the system. In this way, long-lived transition states can also be visited in a simulation run [14]. In our simulation, the parameters were chosen to be χ_{AS}=1.4, χ_{BS}=1.7 for the solvent-polymer interaction, and χ_{AB}=3.0 for the polymer–polymer interaction. These interaction parameters are the same as for the aqueous Pluronic polymer surfactant solution (PL64), previously simulated in [12] and [14].

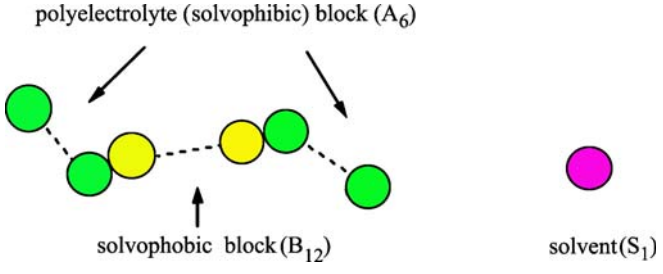

Fig. 1 Schematic representation of the polymer ($A_6B_{12}A_6$) and solvent (S_1) molecules divided into MesoDyn beads

It should be pointed to that, except for the Flory–Huggins parameters, the detailed model we describe here applies to the case where the polyelectrolyte phase behavior is also governed by another Donnan effect, [9] and the interactions between the charged ions are shown by the χ_{IJ}^{D} in salt strength. In a zeroth order approximation $\chi_{IJ}^{D}=\frac{z_I z_J}{C}$, where z_I is the valency of polymer bead I, and C=$2vc_S$ is the number of ions in the reference bath per unit of bead volume. The zeroth order approximation is sufficient for most applications, when the salt strength is high or the polymer charge is low. Apparently, our simulated systems conform to this approximation. Thus, although the Flory–Huggins parameters between different beads are not changed with the increase of charge on the bead A, we think that the interaction between these beads will also be changed due to the Donnan effect in the polyelectrolyte system through χ_{IJ}^{D}.

For all simulations, the dimensionless parameters in the MESODYN program were chosen as (see details in References [15–17]): the time step $\Delta\tau$=50 ns (dimensionless time step $\Delta\tau$=0.5), the noise-scaling parameter Ω=100, the compressibility parameter $K_H^{\prime}=25$, the grid parameter $d=ah^{-1}$=1.1543 (a is the Gaussian bond length), salt strength parameter C=0.1 mol/l, and the total simulation time is 5,000 steps (i.e. 250 us). And all the simulations are on a cubic grid with 32 × 32 × 32 cells of mesh size h. More details of MDDFT are given in [9, 11, 12, 15].

Results and discussion

Mesoscopic structures with different concentration or charges per solvophilic bead

The mesoscale structures are shown in Fig. 2 as a function of block-copolymer concentration and the charge of the solvophilic blocks. These self-assemble aggregates are the structures that the solvophilic A blocks shield the solvophobic B blocks from contact with solvent beads. The A

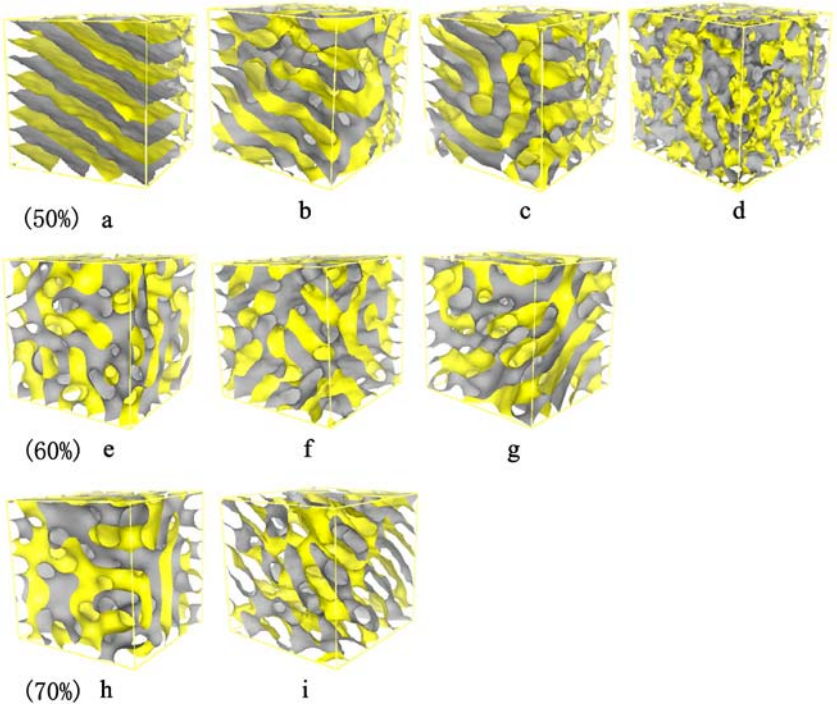

Fig. 2 Snapshots of mesoscale structures (θ_A for mean isosurface level) in polyelectrolyte solution of a triblock copolymer $A_6B_{12}A_6$ for the salt strength parameter 0.1 mol/l at dimensionless time τ=5,000. The parameters varied are the polymer concentration in polymer weight percentage, wt. %, and the charge per A bead, z_A. 50%, isolevel θ_A =0.25: **a** z_A=0, **b** z_A=0.01, **c** z_A=0.02, **d** z_A=0.05; 60%, isolevel θ_A=0.30: **e** z_A=0, **f** z_A=0.2, **g** z_A=0.25; 70%, isolevel θ_A=0.35: **h** z_A=0, **i** z_A=0.35. For 50% system, with increase in the charge of A block, lamellar → defected lamellar→ disorder; other systems (60, 70 and 80%), bicontinuous → defected lamellar→ disorder

concentration is not constant but varies somewhat according to the microenvironment in order to accommodate defect or order structures. The observed phases are lamellar (50%, Fig. 2a), bicontinuous (60%, 70%, Fig. 2e and h) when there is no charge in the A bead. Of course, in our simulation, bicontinuous phases are also found at higher concentrations, such as for 80 and 90% concentration, but they are not shown in this article.

During the simulation, to our surprise, we found that only the 50% copolymer system can form lamellar phase when the charge per A bead is zero, but for other systems, such as 49 or 51%, they can only form disordered or bicontinuous phases, not lamellar aggregates. However, even though the charge per A bead is very small (0.01), the order lamellar structures also become defected: they are perforated by several holes and contain necks between them (Fig. 2b); and a disordered, mesoscopic structure is observed when the charge per A bead is equal to 0.05 (Fig. 2d).

In fact, we heavily concentrated on the change of aggregates in the higher concentration of copolymer when the solvophilic bead has different charges. Bicontinuous phases can be formed for the uncharged copolymer $A_6B_{12}A_6$ in higher concentration, which was used to mimic the phase behavior of the polymer P85 [13] (60%, Fig. 2e; 70%, Fig. 2h), and it is difficult to distinguish with the difference of bicontinuous phases using the isosurface distribution for the different concentrations since there are too many defects. Using the results for uncharged system as a reference we considered the phase behavior relative to a similar polyelectrolyte solution while changing the charge of the A beads for the same concentration of polymer.

In the 60% $A_6B_{12}A_6$ polyelectrolyte solution, we observed the following sequence of mesophases with increasing charge on the A beads: bicontinuous → defected lamellar→ disorder. When the charge of the solvophilic A blocks is small, the system retains the bicontinuous structure of the reference uncharged copolymer surfactant solution (Fig. 2f), then the bicontinuous phase become defected lamellar aggregates (Fig. 2g).

Strictly speaking, these defected lamellae (Fig. 2g) are not similar to an ordered lamellar phase (Fig. 2a). In order to distinguish the difference, the 2D density patterns θ_A are shown in Fig. 3 which were cut through the center of the simulation box. In contrast to the defected lamellar

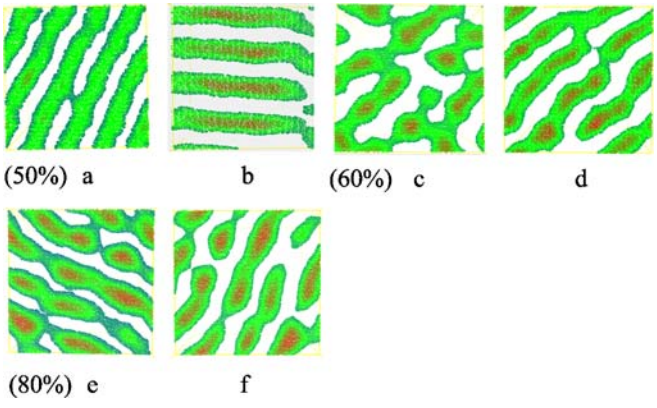

Fig. 3 The density slice of A block in $A_6B_{12}A_6$ solution at dimensionless time τ=5,000. 2D cut through the middle of the box shown in Fig. 2a for **a** (z orientation) and **b** (y orientation); in Fig. 2g for **c** (z orientation) and **d** (y orientation); and for 80% system with the charge of z_A=0.5 for **e** (z orientation) and **d** (y orientation)

structures (Fig. 3c and d, for the 60% system), in which the lamellae are twisted in the defect areas, the ordered lamellae (Fig. 3a and b, for 50% system) are oriented at a certain angle with respect to the normal. We think that the defected lamellar phases are inter-aggregates between the lamellar and bicontinuous phases, because we found that there are some hexagonal holes in the 3D simulation box, which are shown as the red region in the 2D simulation slice (Fig. 3c–f). These mean that the defected lamellar phases may have some properties of the lamellar and bicontinuous phases when the block polymer has some charges. At higher concentrations, the defected lamellar phases can also be found, as shown in the 3D isosurface box (for the 70% system, Fig. 2i) and in the 2D slice (for the 80% system, Fig. 3e and f).

In fact, the bicontinuous and defected lamellar transitions described above are related to the concentration of block polyelectrolyte. At higher concentrations, relatively small charges on the solvophilic block beads do not alter the bicontinuous phase inherent to the uncharged solution. For example, for the 60% system, the disordered mesoscopic structure was found when the charge is only above 0.20; for 70%, 0.4 and for 80%, 0.55. The different phases are summarized in the phase diagram shown in Fig. 4 (we will discuss in the following section). Kyrylyuk and Fraaije [9] have explained the order-to-disorder transitions using the Donnan interaction parameters χ^D, which are similar to the Flory–Huggins interaction parameters used in our simulation. The electrostatic repulsion between charged A blocks leads to changes of the Flory–Huggins interaction parameters χ, and the increase of charge of the block polymer can cause an increase of the Donnan interaction parameters χ^D, which induces a transition from ordered to disordered states. Thus, the Donnan interaction is essential for the phase transition of polyelectrolyte solution. With the range of z_A=0.01~0.7 in our simulations, the variations in the charge or in the salt strength will result in the same phase diagram. These are the reasons that we selected the concentration of polymer to be below 80%, and the salt strength to be 0.1 mol/l. In fact, when we investigated the effect of salt strength on the morphology of polyelectorate, we found that the lamellar aggregates of the 50% uncharged system are not changed in the range of salt strength from 0.1 to 0.4 mol/l. This conclusion is similar the result of [9].

The phase diagram using the order parameter

At the simulation beginning, an homogeneous density distribution was selected, and the phase-separation dynamics from instantaneous quench are characterized by the time evolution of the average order parameter, defined as:

$$p = \overline{\theta - \bar{\theta}^2} = \frac{\int_V \sum_I \left[\theta_I^2(r) - \theta_I^{02}\right] \mathrm{d}r}{V}$$

where p is the mean-squared deviation from homogeneity in the system, which captures both the effects of phase separation and compressibility, and θ is a volume fraction field (which is compared with the experimental weight fraction), V is the volume of cells. The time evolution of p in the first 1,000 simulation steps is shown in Fig. 5. The separation kinetics vary from fast bicontinuous-like nucleation (80%) to slow lamellar phase (50%). From Fig. 5, we find that phase separation can easily take place at higher concentrations of polymer, and can be shown using the order parameters with the increase of the simulation times. One can also find that the higher concentration of the polymer solution, the bigger values of order parameters, and the shorter time of the equilibrium in the simulation. Maybe in higher concentration, the solvophilic A blocks aggregate easily in the solvent, and the interaction between the solvophilic block and solvent beads makes the aggregates form more easily.

Combined with the mesoscale structures discussed above (Fig. 2), the order parameters can be used to draw the phase diagram of polyelectrolyte with increasing charge of the solvophilic block. Fig. 4 shows the relationship between the order parameters and the charge per A bead of polymer $A_6B_{12}A_6$. It should be pointed out that the

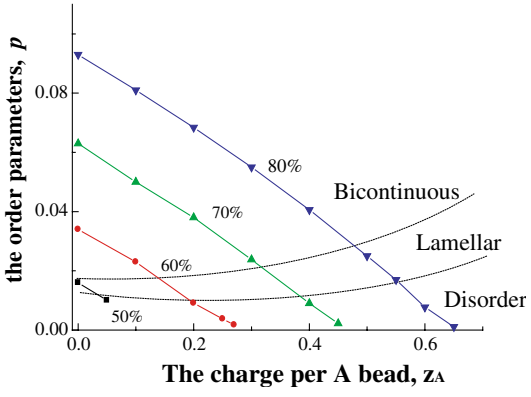

Fig. 4 The phase diagram of polymer $A_6B_{12}A_6$ in concentrated concentration when solvophilic A bead has different charges

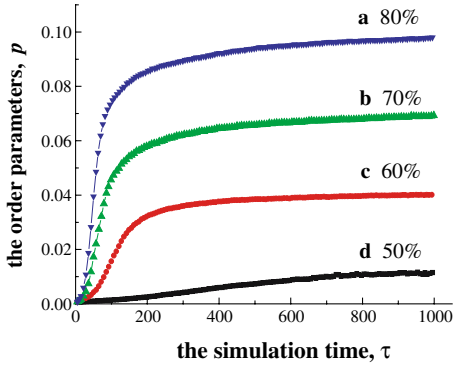

Fig. 5 Time evolution of dimensionless order parameter p (see test for definition) in polymer surfactant solutions. At dimensionless time τ=0 the system is quenched from homogeneous density distribution. The labels a–g refer to simulations of **a** 80%, **b** 70%, **c** 60%, **d** 50%

lamellar region between bicontinuous and disordered regions should be a defected lamellar phase, not ordered lamellar aggregates as in Fig. 2a. In fact, this region is very small from the bicontinuous to disorder transitions with the increase of charge of solvophilic block A for any polyelectrolyte solution. The simulation results show that the order parameter can be considered as an adjunct for the mesoscale structures, and for other similar investigations, maybe we can deduce the mesoscale phases using the values of the order parameters.

Conclusion

The MESODYN method can be used to simulate experimental conditions to investigate the instantaneous quench from homogeneous density distribution for polyelectrolyte solutions. Using the simulation, the time scale of phase separation can be predicted on a short time scale, unlike the real experiments, in which the phase separation must continue several days, or even weeks of equilibration time. At higher concentration (above 50% systems), relatively small charges on the solvophilic block do not alter the bicontinuous phase inherent to uncharged solution for $A_6B_{12}A_6$, and at moderate concentrations (50% system), even though the charge per solvophilic bead is very small, the order lamellar structures become defected. At high charges per bead, disordered, mesoscopic structures can be formed for any simulation system. Another finding is that the value of the order parameter can be used to predict the mesoscale phases formed in the solution. One conclusion is that mesoscopic simulations can be considered as an adjunct to experiments and provide other valuable information for experiment.

Acknowledgement This work was supported by the National Science Foundation of China (20303011 and 20473047).

References

1. Shi AC, Noolandi J (1999) Macromol Theory Simul 8:214–229
2. Muthukumar M (2002) Macromolecules 35:9142–9145
3. Liu S, Ghosh K, Muthukumar M (2003) J Chem Phys 119:1813–1823
4. Ermoshikin AV, Olevra de la Gruz M (2003) Macromolecules 36:7824–7832
5. Sfika V, Tsitsilianis C (2003) Macromolecules 36:4983–4988
6. Cameron NS, Eisenberg A, Brown GR (2002) Biomacromolecules 3:124–132
7. Förster S, Hermsdorf N, Leube W, Schnablegger H, Regenbrecht M, Akari S, Lindman P, Böttcher C (1999) J Phys Chem B 103:6657–6668
8. Regenbrecht M, Akari S, Förster S, Möhwald H (1999) J Phys Chem B 103:6669–6675
9. Kyrylyuk AV, Fraaije JGEM (2004) J Chem Phys 121:2806–2812
10. Borisov OV, Zhulina EB (2003) Macromolecules 36:10029–10036
11. Fraaije JGEM, van Vlimmeren BAC, Maurits NM, Postrma M, Evers OA, Hoffmann C, Altevogt P, Goldbeck-Wood G (1997) J Chem Phys 106:4260–4269
12. van Vlimmeren BAC, Maurits NM, Zvelindovsky AV, Sevink GJA, Fraaije JGEM (1999) Macromolecules 32:646–656
13. Lam YM, Goldbeck-Wook G (2003) Polymer 44:3593–3605
14. Horvat A, Lyakhova KS, Sevink GJA, Zvelindovsky AV, Magerle R (2004) J Chem Phys 120:1117–1126
15. Sevink GJA, Fraaije JGEM, Huinink HP (2002) Macromolecules 35:1848–1859
16. Fraaije JGEM (1993) J Chem Phys 99:9202–9212
17. Kyrylyuk AV, Zvelindovsky AV, Sevink GJA, Fraaije JGEM (2002) Macromolecules 35:1473–1476